The Astrophysical Journal Letters, 804:L41 (5pp), 2015 May 10 doi:10.1088/2041-8205/804/2/L41

INERTIAL RANGE TURBULENCE OF FAST AND SLOW SOLAR WIND AT 0.72 AU AND SOLAR MINIMUM

Eliza Teodorescu[1], Marius Echim[1,2], Costel Munteanu[1,6,7], Tielong Zhang[3], Roberto Bruno[4], and Peter Kovacs[5]
[1] Institute for Space Sciences, Măgurele, Romania; eliteo@spacescience.ro
[2] Belgian Institute for Space Aeronomy, Bruxelles, Belgium
[3] Space Research Institute, Graz, Austria
[4] INAF-IAPS, Istituto di Astrofizica e Planetologia Spaziali, Rome, Italy
[5] Geological and Geophysical Institute of Hungary, Budapest, Hungary
[6] University of Bucharest, Măgurele, Romania
[7] University of Oulu, Oulu, Finland
Received 2015 February 20; accepted 2015 April 22; published 2015 May 11

ABSTRACT

We investigate *Venus Express* observations of magnetic field fluctuations performed systematically in the solar wind at 0.72 Astronomical Units (AU), between 2007 and 2009, during the deep minimum of solar cycle 24. The power spectral densities (PSDs) of the magnetic field components have been computed for time intervals that satisfy the data integrity criteria and have been grouped according to the type of wind, fast and slow, defined for speeds larger and smaller, respectively, than 450 km s^{-1}. The PSDs show higher levels of power for the fast wind than for the slow. The spectral slopes estimated for all PSDs in the frequency range 0.005–0.1 Hz exhibit a normal distribution. The average value of the trace of the spectral matrix is −1.60 for fast solar wind and −1.65 for slow wind. Compared to the corresponding average slopes at 1 AU, the PSDs are shallower at 0.72 AU for slow wind conditions suggesting a steepening of the solar wind spectra between Venus and Earth. No significant time variation trend is observed for the spectral behavior of both the slow and fast wind.

Key words: interplanetary medium – magnetic fields – plasmas – solar wind – turbulence

1. INTRODUCTION

The spectral properties of the magnetic field and plasma fluctuations in the solar wind have been investigated in situ over several decades for a broad range of frequencies and various radial distances. It has been found that the power spectral density (PSD) of magnetic field fluctuations exhibits three different power-law regimes, $P(k) = P_0 k^{-\alpha}$, characterized by different exponents: (i) $\alpha \approx -1$ for smaller k (e.g., Matthaeus & Goldstein 1986; Verdini et al. 2012); (ii) $\alpha \approx -5/3$ for the intermediate k (e.g., Marsch & Tu 1990), this range of k is also anisotropic and the fluctuations parallel and perpendicular to the magnetic field may exhibit a different power-law index (see, e.g., Dasso et al. 2005; Horbury et al. 2012); and (iii) $\alpha \leqslant -2.5$ with a minimum index close to −4.5 (Leamon et al. 1999; Bruno et al. 2014) for the largest k (see, also, Coleman 1968; Stawicki et al. 2001, and Bruno & Carbone 2013; Alexandrova et al. 2013, for a review). Frisch (1995) described the three characteristic power-law regimes, separated by spectral breaks, as the magnetohydrodynamic equivalents of the scale ranges of classical hydrodynamic turbulence: (i) the driving (or energy containing) range; (ii) the inertial range, dominated by nonlinear turbulent interactions which transfer the energy over multi-scales; and (iii) the dissipation range. The physical processes contributing to dissipation in turbulent collisionless plasmas are still an open issue and in recent years it has been argued (see, e.g., Alexandrova et al. 2013) that below proton scales, another turbulent cascade may take place which is described by a different power law. This is followed by an exponential law which could be indicative of dissipation.

In practice, the analysis of an in situ time series provides PSD as a function of frequency in the spacecraft reference frame, $P(f_{sat})$, which would correspond to the Doppler-shifted wavevector spectra, $P(k)$, under the assumption that the plasma flows over the spacecraft much faster than the characteristic time evolution of the nonlinearly interacting turbulent spatial structures/eddies (the Taylor hypothesis). In the solar wind, the transition between the driving and inertial ranges is generally observed at frequencies between 10^{-4} and 10^{-3} Hz which would correspond to spatial scales related to the solar wind correlation/integral length (λ) or the typical size of the "energy containing eddies" (Batchelor 1970; Matthaeus et al. 1994). The high-frequency limit of the inertial range in the solar wind and the transition to the kinetic regime is marked by a break in the spacecraft-frame frequency representation, generally in the vicinity of spatial scales (under the Taylor hypothesis) of the order of the proton inertial length or the proton Larmor radius (e.g., Chen et al. 2014). Recently, the variation of this break with heliocentric distance was discussed by Bruno & Trenchi (2014). High-resolution data seem to suggest that dissipation may effectively start at higher frequencies corresponding to the electron Larmor radius (Alexandrova et al. 2009). The solar wind is a supersonic and super-Alfvénic tenuous stream of collisionless plasma emerging from the dynamic solar corona, and therefore discerning "pure" turbulence features from other structures convected from the Sun is still an issue (see, for instance, Tu & Marsch 1995; Bruno et al. 2007; Borovsky 2008).

Solar wind observations in the inner heliosphere (between 0.3 and 0.9 AU) suggest that the ordering parameter of turbulent properties is the "age" of the turbulence, evaluated as the time it takes for the solar wind to travel from the Sun to the spacecraft, rather than the radial distance. The "aging" of the solar wind turbulence is also characterized by a progressive spectral dominance of the "2D" mode of the turbulence (characterized mainly by perpendicular wavevectors) over the "slab" mode (dominated mainly by parallel wavevectors; Ruiz et al. 2011). Analyses based on a global mean magnetic field estimate concluded that the slow wind generally exhibits features of "2D" turbulence, while the turbulence in the fast

wind is more of the "slab" type (Dasso et al. 2005; Weygand et al. 2011) and the anisotropic state found near the Sun evolves toward a more isotropic state at 1 AU. On the other hand, approaches exploring anisotropy through the scale-dependent local mean magnetic field (e.g., Horbury et al. 2008; Podesta 2009; Wicks et al. 2010; Forman et al. 2011) indicate that the high-speed solar wind power spectrum is dominated by perpendicular "2D" fluctuations. Simulation results (Chen et al. 2011) show the same discrepancy between the global and local mean magnetic field approaches and the authors conclude that global mean magnetic field scaling is not able to properly discriminate between parallel and perpendicular fluctuations. Smith (2003) shows that at high latitudes, roughly equal proportions of slab (1D) and 2D coexist in the same plasma element.

At solar minimum, the solar wind is characterized by an increased recurrence of high-speed streams (up to 800 km s^{-1} and more) with lower density and higher temperature, whose origin is the meridional extensions of the polar coronal holes. The properties of fast and slow wind turbulence were investigated for different phases of the solar cycle from data recorded by *Helios* (Bavassano & Bruno 1989, 1991; Ruiz et al. 2011), *ACE* (Borovsky 2012b), *Ulysses* (Yordanova et al. 2009), *Cluster*, THEMIS (Weygand et al. 2011), *Messenger*, and *Wind* (Bruno & Trenchi 2014; Bruno et al. 2014). Observations of the solar wind by *Ulysses* at larger radial distances (between 1.5 and 5.4 AU), outside the ecliptic and close to the solar minimum, show that the spectral index of the fast wind inertial range turbulence presents values in the range $-1.79 < \alpha < -1.55$ for the magnetic field components, and between $-1.52 < \alpha < -1.25$ for the total field, $|B|$. The spectra of the slow wind exhibit similar power-law behavior but with steeper slopes, $-1.95 < \alpha < -1.45$ for the components of the magnetic field and $-1.78 < \alpha < -1.55$ for the total field (Yordanova et al. 2009). It is unclear whether or not the inertial range spans roughly the same frequency range for the fast and slow wind.

In situ observations at 1 AU indicate that the *median* of the magnetic spectral index in the inertial range depends on the type of wind: it is shallower for the fast wind ($V_{\rm wind} > 450$ km s^{-1}), $\overline{\alpha} = -1.54$, compared to the slow wind, $\overline{\alpha} = -1.70$, as shown by Borovsky (2012a) from 10 years of *ACE* data (1998–2008). The spectral index may assume "extreme" values, larger than −1.33 and smaller than −1.95. Steeper spectral slopes are observed at 1 AU when the solar wind density is larger, the temperature is smaller, the speed takes on lower values, and the number of strong directional discontinuities is reduced (Borovsky 2012a). Close to the high-frequency limit of the inertial range, at proton scales, in the vicinity of the fluid/kinetic spectral break, *Wind* (at 0.99 AU) and *Messenger* (at 0.42 AU) data show that the spectral slope may depend on the power density in the inertial range: steeper slopes are observed for larger power in the inertial subrange (Bruno et al. 2014). This frequency break moves toward smaller frequencies as the radial distance increases (Bruno & Trenchi 2014).

2. SPECTRAL PROPERTIES OF FAST AND SLOW SOLAR WIND AT 0.72 AU

We analyze data recorded by *Venus Express* (*VEX*) in the solar wind in the vicinity of Venus, at 0.72 AU, between 2007 January and 2009 December, during the minimum of solar cycle 24. Since Venus has no intrinsic magnetic field, its induced magnetosphere is confined to shorter distances from the planet, and thus *VEX* spends more than 20 hr each day of the year in the solar wind. Thus, *VEX* is a unique solar wind monitor which investigates the inner heliospheric solar wind on a day to day basis for almost one solar cycle, since 2006. The turbulent fluctuations of the solar wind magnetic field considered in this study are provided by the *VEX* Magnetometer (*VEX*-MAG; Zhang et al. 2006) with a cadence of 1 Hz. The data are obtained through an offline calibration procedure by donwsampling the 32 Hz resolution data.

The plasma state (electron and ion spectra and their moments, e.g., density, temperature, velocity) is investigated using the Analyzer of Space Plasma and Energetic Atoms (ASPERA, Barabash et al. 2007). ASPERA operates in the solar wind for short time intervals of the order of one to two hours, close to the orbit apogee. The ion and electron spectra and their moments are provided with a time resolution of 196 seconds which does not allow for a spectral analysis of the solar wind plasma parameters. Nevertheless, the estimate of the moments of the ion velocity distribution function provides us with the data we need to select high and low speed solar wind. Inspired by previous studies, we select the slow and fast wind intervals based on a threshold speed value equal to 450 km s^{-1}. The magnetic field experiment operates continuously, however, we consider time intervals of roughly four hours, which are close to the *VEX* apogee and include those time periods when ASPERA is also operating.

Several quality checks impose additional constraints on the magnetic field data analysis. We disregard the time intervals shorter than 1 hr and those with data gaps exceeding 30 consecutive points. In general, the total missing data points amount to less than 3% of the total number of samples for the selected time intervals and they appear to be randomly distributed over time. Thus, the number of data gaps in the selected time intervals is small and their lengths are short. A linear interpolation is applied prior to the spectral analysis. From a total of 1094 orbits between 2007 January and 2009 December, only 204 time intervals fulfill the data quality requirements, 48 of which correspond to fast solar wind observations ($V_{\rm wind} > 450$ km s^{-1}).

The magnetic field components are provided in the Venus Solar Orbital (VSO) rectangular frame, with the Ox axis aligned in the Sunward direction and the Oz axis perpendicular to the ecliptic plane in the northward direction. The PSDs are computed with a Welch algorithm (Welch 1967) averaging periodograms applied on B_x, B_y, B_z, and the total field, $|B|$, for all of the selected time intervals. We also compute the trace of the spectral matrix of the fluctuations. A summary plot of all the power spectra is provided in Figure 1; different colors illustrate different types of wind (fast/slow) and different years. An average spectrum is computed as an ensemble average of all the spectra for the fast and slow solar wind, respectively.

The spectral power of the fast solar wind is systematically larger than for the slow wind, as shown by previous results in other locations of the heliosphere (see the review by Bruno & Carbone 2013 and recent results at 0.38 and 1 AU by Bruno et al. 2014). The PSDs exhibit a power-law regime in the frequency range $[5 \times 10^{-3}, 10^{-1}]$ Hz. A change in the spectral slope is observed around 0.2–0.3 Hz, close to the local Doppler-shifted proton gyrofrequency, followed by a frequency range showing a steepening of the spectra which could

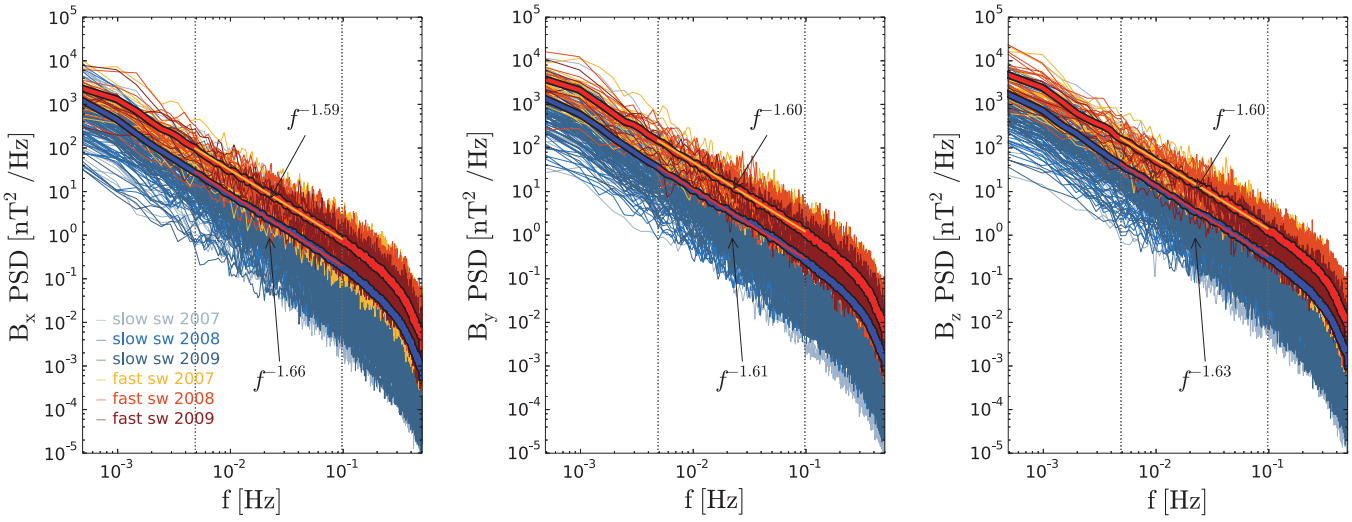

Figure 1. Summary plot of the power spectral density spectrum of B_x, B_y, and B_z from *VEX* magnetic field data recorded between 2007 and 2009, during the minimum of the 24th solar cycle. Yellow and red lines correspond to fast solar wind, gray and blue lines correspond to slow solar wind. The black dotted lines mark the frequency interval for which the spectral index of each spectrum is computed. An average spectrum is derived as an ensemble average of all the spectra obtained for the fast (the embossed red line) and slow wind (the embossed blue line), respectively. The spectral slope of the average spectra is computed for the frequency range marked by yellow and magenta, respectively.

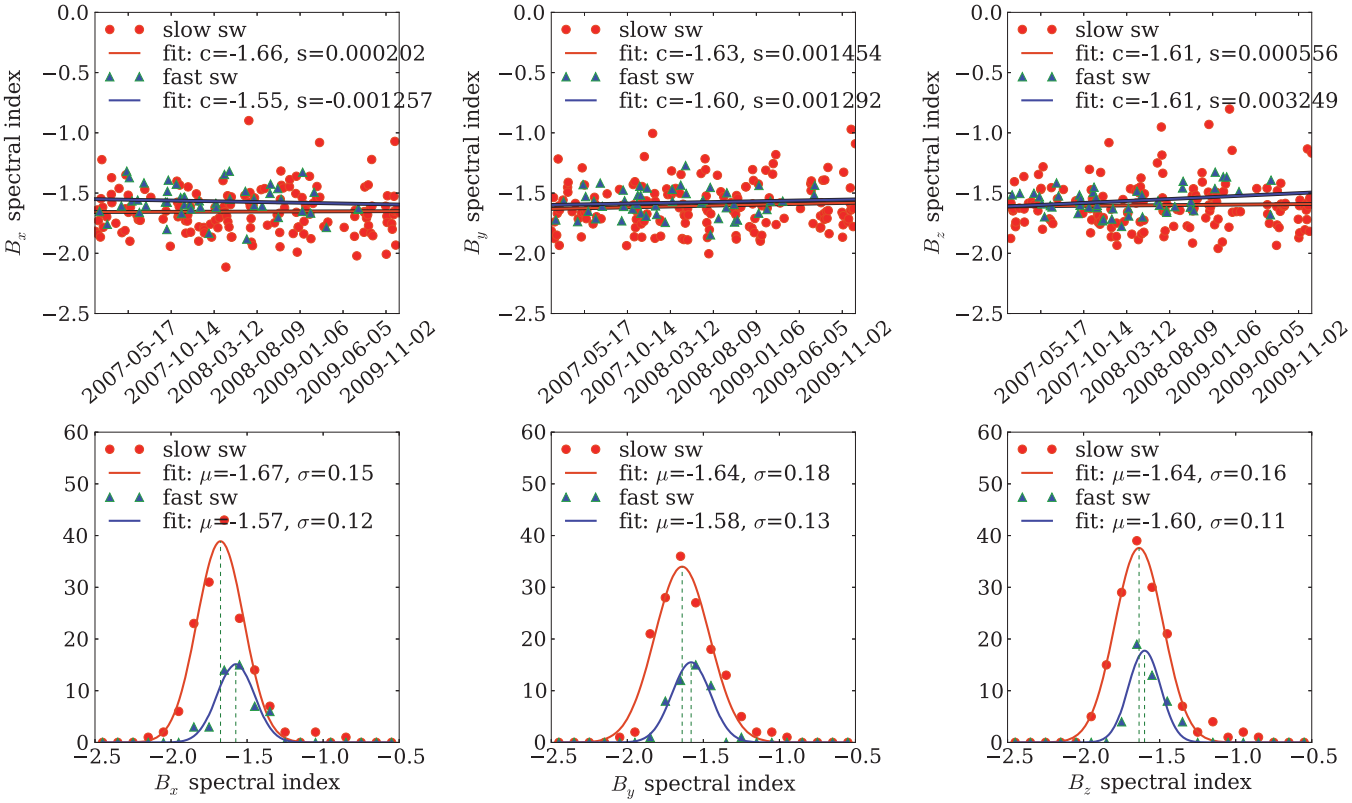

Figure 2. Distribution of spectral index for B_x, B_y, and B_z from data recorded between 2007 and 2009. Upper row: evolution in time of the spectral indices computed in the frequency interval indicated in Figure 1. c is the constant (intercept) of the first degree polynomial linear fit and s is the slope of the fit. Lower row: the histogram of the spectral indices approaches a Gaussian distribution with a mean close to −5/3 for the slow wind and −1.6 for the fast wind.

correspond to the lowest frequencies of the non-MHD kinetic turbulent cascade. In order to minimize the effect of inherent uneven sampling of the frequency range by the periodogram technique, the spectral index/slope has been computed from PSDs rebinned and averaged over equal logarithmic bins of frequency. In addition to rebinning the frequency range, we have also searched for power-law behavior by varying the limits of the fitting frequency range. Thus, for each of the power spectra, the spectral index (or slope) is calculated by a linear least-square fit over the interval $[5 \times 10^{-3}, 10^{-1}]$ Hz. This range would correspond to the high-frequency part of the inertial subrange at 0.72 AU and solar minimum. The number of data intervals is sufficiently large to allow for a statistical analysis of the distribution of the spectral indices obtained at

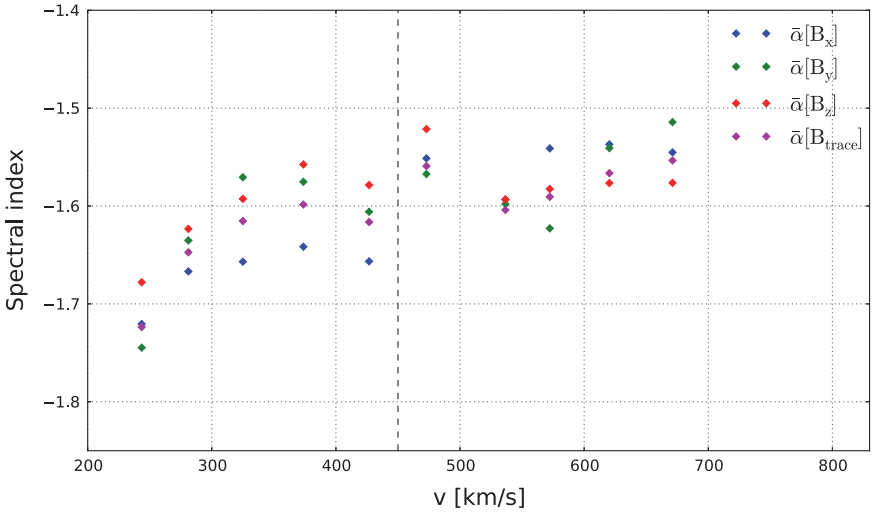

Figure 3. Spectral index as a function of solar wind speed; we show averages over velocity bins of 50 km s^{-1} width. Different colors ilustrate different magnetic field components. Data is collected in the solar wind by VEX between 2007 and 2009. The dotted vertical line represents the threshold we chose to select fast and slow solar wind.

solar minimum, between 2007 and 2009, as illustrated by Figure 2.

The a priori separation of fast from slow solar wind allows for the independent and simultaneous tracking of the evolution of the spectral properties of turbulence for the two types of wind. The least-squares linear fitting of the distributions of the spectral slopes (upper panels of Figure 2) provides experimental evidence that the spectral indices do not exhibit any temporal trends over the years while the solar minimum deepens, both for the slow and fast solar wind. This can be considered as an indication that the processes contributing to the power-law scaling are mainly local, possibly related to nonlinear interactions leading to the turbulent transfer of energy between scales. The histograms of the spectral indices show that the slopes of the magnetic field power spectra in the inertial range fit a Gaussian distribution, as seen in the lower row of plots in Figure 2. The three components of the magnetic field exhibit different average spectral slopes for the fast and slow wind: $\bar{\alpha}_x^{\rm fast} = -1.57 \pm 0.02$, $\bar{\alpha}_y^{\rm fast} = -1.58 \pm 0.02$, and $\bar{\alpha}_z^{\rm fast} = -1.60 \pm 0.02$, and $\bar{\alpha}_x^{\rm slow} = -1.67 \pm 0.01$, $\bar{\alpha}_y^{\rm slow} = -1.64 \pm 0.01$, $\bar{\alpha}_z^{\rm slow} = -1.64 \pm 0.01$, respectively, where $\bar{\alpha}_i^{\rm fast/slow}$ indicates the mean spectral index of the component i and the fast or slow type of wind. The mean spectral index of the trace of the spectral matrix (not shown) varies from $\bar{\alpha}_B^{\rm fast} = -1.60 \pm 0.01$ in the fast wind to $\bar{\alpha}_B^{\rm slow} = -1.65 \pm 0.01$ in the slow wind.

The variation of the spectral index as a function of the solar wind speed is shown in Figure 3. The average spectral indices of the magnetic field become shallower with increasing plasma velocity, which is in good agreement with previous work (Chen et al. 2013). The continuous trend also seems to indicate that the solar wind velocity may be a controlling parameter for the spectral slope. Nevertheless, recent studies indicate that cross-helicity is equally important in controlling the spectral behavior (Chen et al. 2013).

The *VEX* results show similarities with the spectral analysis of *Wind* magnetic field data at 1 AU during roughly the same time interval, between 2004 June and 2009 April. Data from *Wind* showed a mean spectral slope from −1.6 (for wind speeds larger than 600 km s^{-1}) to −1.72 (for speeds smaller than 400 km s^{-1}; Chen et al. 2013). Another analysis of solar wind turbulence at 1 AU, based on *ACE* data recorded between 1998 and 2008, suggests a median spectral slope of the magnetic field equal to −1.54 for speeds larger than 550 km s^{-1} and −1.70 for speeds smaller than 450 km s^{-1}, respectively (Borovsky 2012a). Nevertheless, the *VEX* data suggest that, on average, the slopes of the slow wind spectra are shallower at 0.72 AU than at 1 AU, while the fast wind shows, on average, comparable slopes. We note the differences between the mean spectral slopes of the three magnetic field components for the slow wind conditions and roughly the same mean slope for the fast wind. On the other hand, more spectral power is observed for the B_y and B_z components in the fast wind. This is in agreement with our expectation of finding more power in the perpendicular components than the parallel components, as fast wind is more Alfvénic and Alfvénic fluctuations are mainly perpendicular to the local mean magnetic field and are not compressive. At 0.72 AU, the Parker spiral (mean field) for the fast (700 km s^{-1}) solar wind would be around 24°, which is not far from the X direction in the VSO reference system. Thus, more power should be expected for the Y and Z components of the magnetic field (Klein et al. 1993). The anisotropy will be the subject of a future study on the same data set.

3. DISCUSSION AND CONCLUSIONS

We have investigated the spectral behavior of the solar wind magnetic field at 0.72 AU for low solar activity between 2007 and 2009 using data provided by *VEX*. The PSDs of the magnetic field components and the trace of the spectral matrix indicate that the inertial range of turbulence can be identified as power-law behavior in the fast and slow solar wind. More power is contained in the fast wind spectra which also exhibit shallower slopes than the slow wind. The mean value of the slope assumes values around -1.6 ± 0.01 for the fast wind and -1.65 ± 0.01 for the slow wind, respectively. Our results fully agree with general predictions found in the literature concerning different spectral slopes of magnetic field fluctuations depending on solar wind conditions.

In particular, Chen et al. (2013) clearly showed how the spectral index of the magnetic field and velocity fluctuations depend on their Alfvénicity, which can be expressed by the normalized cross-helicity σ_C. These authors, analyzing five years of *Wind* data, found that as σ_C decreases, the magnetic energy starts to dominate the kinetic energy, and the magnetic field spectrum becomes steeper than the velocity spectrum, in line with predictions (Müller and Grappin 2005, among others). The tendency for the magnetic spectrum to dominate over the kinetic is a natural outcome for stationary, critically balanced MHD turbulence (Goldreich & Sridhar 1995) generated by nonlinear interacting Alfvén waves (Gogoberidze et al. 2012). Consequently, since we study fast and slow wind, which differ in Alfvénicity (Bruno & Carbone 2013), with the fast wind being more Alfvénic than slow wind, we should expect to find magnetic field spectra in the fast wind less steep than those in slow wind. In addition, a comparison with similar data at 1 AU suggests that, on average, the spectra steepen while the slow solar wind is transported between 0.72 and 1 AU, suggesting that nonlinear interactions are at work. On the other hand, the fast wind exhibits less clear evidence of radial steepening.

The solar wind magnetic field spectral indices between 2007 and 2009 have a normal distribution. We do not find a significant temporal trend in the slopes. The average spectral slopes of the three magnetic components suggest an anisotropic repartition of power. There is evidence for a change in the spectral slope in the vicinity of the proton cyclotron radius, possibly associated with the transition from the inertial to the kinetic subrange.

Our results suggest that at 0.72 AU and solar minimum, the slow wind exhibits, on average, spectral behavior closer to the "$f^{-5/3}$" law with some differences between the mean slopes of the magnetic field components. Thus, there are indications that the turbulence is anisotropic and models based on the isotropy hypothesis, like Kolmogorov (1941) and/or Iroshnickov–Kraichnan, are not applicable. Modern theories of anisotropic strong MHD turbulence (Goldreich & Sridhar 1995) predict that the perpendicular spectrum of turbulence may approach for some conditions the "$f^{-5/3}$" scaling. In the absence of resolute plasma measurements from *VEX,* we can only suggest that the slow wind spectra are perhaps dominated by the perpendicular component. Nevertheless, the younger turbulence carried by the fast wind is described by shallower spectral slopes which show a tendency to approach asymptotically a "$f^{-3/2}$" power law. This could possibly signify that the structure of the turbulence exhibits features consistent with models of anisotropic turbulence as in Boldyrev (2006). In other words, our results may suggest that the slow wind at 0.72 AU and solar minimum is dominated by filament-like structures at the smallest scales (as suggested by Goldreich & Sridhar 1995), while the fast wind turbulence is dominated by sheet-like structures at the smallest scales (as suggested by Boldyrev 2006), possibly related to phenomenological turbulent features of the solar wind at the origin, in the corona.

Research supported by the European Community's Seventh Framework Programme (FP7/2007-2013) under grant agreement No. 313038/STORM, and a grant of the Romanian Ministry of National Education, CNCSUEFISCDI, project No. PN-II-ID-PCE-2012-4-0418. The data analysis was partially performed with the AMDA science analysis system provided by the Centre de Donnes de la Physique des Plasmas (IRAP, Universit Paul Sabatier, Toulouse) supported by CNRS and CNES.

REFERENCES

Alexandrova, O., Saur, J., Lacombe, C., et al. 2009, PhRvL, 103, 16
Alexandrova, O., Chen, C. H. K., Sorriso-Valvo, L., Horbury, T. S., & Bale, S. D. 2013, SSRv, 178, 101
Batchelor, G. K. 1970, The Theory of Homogeneous Turbulence (Cambridge: Cambridge Univ. Press)
Barabash, S., Sauvaud, J.-A., Gunell, H., et al. 2007, P&SS, 55, 1772
Bavassano, B., & Bruno, R. 1989, JGR, 94, 168
Bavassano, B., & Bruno, R. 1991, JGR, 96, 1737
Boldyrev, S. 2006, PhRvL, 96, 115002
Borovsky, J. E. 2008, JGR, 113, A8
Borovsky, J. E. 2012a, JGR, 117, A5
Borovsky, J. E. 2012b, JGR, 117, A6
Bruno, R., & Carbone, V. 2013, LRSP, 10, 2
Bruno, R., D'Amicis, R., Bavassano, B., Carbone, V., & Sorriso-Valvo, L. 2007, AnGeo, 25, 1913
Bruno, R., & Trenchi, L. 2014, ApJL, 787, L24
Bruno, R., Trenchi, L., & Telloni, D. 2014, ApJL, 793, L15
Chen, C. H. K., Bale, S. D., Salem, C. S., & Maruca, B. A. 2013, ApJ, 770, 125
Chen, C. H. K., Leung, L., Boldyrev, S., Maruca, B. A., & Bale, S. D. 2014, GeoRL, 41, 8081
Chen, C. H. K., Mallet, A., Yousef, T. A., Schekochihin, A. A., & Horbury, T. S. 2011, MNRAS, 415, 3219
Coleman, P. J., Jr. 1968, ApJ, 153, 371
Dasso, S., Milano, L. J., Matthaeus, W. H., & Smith, C. W. 2005, ApJL, 635, L181
Gogoberidze, G., Chapman, S. C., & Hnat, B. 2012, PoP, 19, 2310
Goldreich, P., & Sridhar, S. 1995, ApJ, 438, 763
Forman, M. A., Wicks, R. T., & Horbury, T. S. 2011, ApJ, 733, 76
Frisch, U. 1995, Turbulence (Cambridge: Cambridge Univ. Press)
Horbury, T. S., Forman, M., & Oughton, S. 2008, PhRvL, 101, 175005
Horbury, T. S., Wicks, R. T., & Chen, C. H. K. 2012, SSRv, 172, 325
Kolmogorov, A. 1941, DoANT, 30, 301
Klein, L., Bruno, R., Bavassano, B., & Rosenbauer, H. 1993, JGR, 98, A10
Leamon, R. J., Smith, C. W., Ness, N. F., & Wong, H. K. 1999, JGR, 104, 22331
Marsch, E., & Tu, C.-Y. 1990, JGR, 95, 11945
Matthaeus, W. H., & Goldstein, M. L. 1986, PhRvL, 57, 495
Matthaeus, W. H., Oughton, S., Pontius, D. H., Jr, & Zhou, Y. 1994, JGR, 99, 19267
Müller, W.-C., & Grappin, R. 2005, PhRvL, 95, 114502
Podesta, J. J. 2009, ApJ, 698, 986
Ruiz, M. E., Dasso, S., Matthaeus, W. H., Marsch, E., & Weygand, J. M. 2011, JGR, 116, A10
Smith, C. W. 2003, in AIP Conf. Proc. 679, Astronomy and Astrophysics, ed. M. Velli, R. Bruno, & F. Malara (New York: AIP), 413
Tu, C.-Y., & Marsch, E. 1995, SSRv, 73, 1
Stawicki, O., Gary, S. P., & Li, H. 2001, JGR, 106, 8273
Verdini, A., Grappin, R., Pinto, R., & Velli, M. 2012, ApJL, 750, L33
Weygand, James M., Matthaeus, W. H., Dasso, S., & Kivelson, M. G. 2011, JGR, 116, A8
Welch, P. D. 1967, IEEE Trans. Audio Electroacoustics, AU-15, 70
Wicks, R. T., Horbury, T. S., Chen, C. H. K., & Schekochihin, A. A. 2010, MNRAS, 407, L31
Yordanova, E., Balogh, A., Noullez, A., & von Steiger, R. 2009, JGR, 114, A8
Zhang, T., Baumjohann, W., Delva, M., et al. 2006, P&SS, 54, 1336